Astron. Astrophys. 317, 845–858 (1997)

ASTRONOMY
AND
ASTROPHYSICS

Carbon isotope ratio in carbon stars of the galactic halo

W. Aoki [1,2] **and T. Tsuji** [1]

[1] Institute of Astronomy, The University of Tokyo, 2-21-1, Osawa, Mitaka 181, Japan
[2] Department of Astronomy, School of Science, The University of Tokyo, Bunkyo-ku, Tokyo 113, Japan

Received 16 January 1996 / Accepted 5 May 1996

Abstract. We analysed CN red system ($\sim$8000 Å) and C_2 Swan system ($\sim$4700 Å) to know carbon isotope ratios ($^{12}C/^{13}C$) for carbon stars in the Galactic halo, named CH stars. The isotope ratios are obtained for 6 CH stars by the curve-of-growth analysis of the isolated ^{12}CN and ^{13}CN lines. In this analysis, we compared directly ^{12}CN and ^{13}CN lines of similar intensities (iso-intensity method), and the resulting $^{12}C/^{13}C$ ratios are almost independent of the model atmosphere and its parameters. The ^{13}CN lines appear to be too weak in some CH stars, for which we applied the spectral synthesis method to the stronger C_2 Swan band, obtained $^{12}C/^{13}C$ ratios for two stars and estimated the lower limits of $^{12}C/^{13}C$ ratios for two stars. In this case, however, the results depend on model atmosphere and its parameters. Results from our present and previous works show that most of them (12 stars) distribute around $^{12}C/^{13}C \sim 10$ and two stars have very high values ($^{12}C/^{13}C \geq 500$). The distribution of $^{12}C/^{13}C$ ratios in CH stars is different from that of the population I carbon stars as well as population II oxygen-rich giants (G$\sim$K types). The CH stars of very high $^{12}C/^{13}C$ ratios can be explained by dredge-up of ^{12}C due to 3α-process as in population I carbon stars (N-type). On the other hand the formation of the CH stars with low $^{12}C/^{13}C$ ratios requires the large supply of ^{12}C followed by a process of decreasing $^{12}C/^{13}C$ ratio.

Key words: stars: abundances – stars: carbon – stars: population II – stars: AGB and post AGB – Galaxy: halo

1. Introduction

During the early evolution of the Galaxy, stellar nucleosynthesis played an important role, since it produced all the elements other than a few light elements (H, D, ^{3}He, ^{4}He, ^{7}Li), if the standard big-bang theory is correct. The role played by massive halo stars can be known only indirectly through the surface chemical composition of long-lived low mass halo stars formed by the ejecta of the massive halo stars, and it is now realized that the elements from the stable α nuclei including oxygen to the iron group have been produced in the massive stars that exploded as the types I and II supernovae. How about the intermediate-mass stars which may have produced carbon, nitrogen, and some heavy (the s-process) elements in their red giant branch (RGB) and asymptotic giant branch (AGB) phases? In principle, the products of these evolutionary phases can also be traced by the surface chemical compositions in the low mass halo stars formed from the interstellar matter enriched by the mass-loss of the intermediate-mass halo stars. However, the interstellar matter at this time has been already polluted by the ejecta of many generations of more massive stars and interpretation on chemical analyses of the low mass halo stars formed in this way may be by no means easy. In fact, the origin of carbon, nitrogen, and heavy elements in the Galactic chemical evolution is not yet very clear.

On the other hand, more direct information on the role of the intermediate-mass stars of the halo can be found in the halo red giant stars and especially in the CH stars, carbon-rich stars of population II, first recognized by Keenan (1942). CH stars should be important for the chemical evolution of the early Galaxy because they are a great part of evolved stars in metal-poor system like the Galactic halo. For example, Hartwick & Cowley (1985) suggested that the ratio of the local density of CH stars is as high as 30% of metal-poor giants. CH stars are characterized by strong G band of CH, very weak metal lines and enhanced lines of the s-process elements. The excesses of carbon and the s-process elements such as Ba and Sr are the characteristics which are found in AGB stars. However as shown by the analysis of HD26 and HD201626 (Wallerstein & Greenstein 1964), the absolute magnitudes of CH stars are too low to be AGB stars. To explain this contradiction a model of mass transfer from carbon star to its companion have been considered. In this model it is thought that the carbon star has evolved to white dwarf and now cannot be detected, while the companion has evolved to giant and is observed as CH star. In fact a great part of CH stars has been shown to be binary by McClure & Woodsworth (1990). According to this model these stars may have conserved the products of carbon-rich primary and survive until the present in the Galactic halo.

We have tried to know carbon isotope ratios of CH stars to restrict their evolutionary models. Carbon isotope ratio is

Table 1. Observations

	Star Name	V	RV(km/s)	Date	S/N	Ref.[a]
7790 Å$\sim$ 8030 Å	HD224959	9.50	-132	1992/9/2	61	1
	HD198269	8.23	-207	1992/9/2,3	167	1
	HD85066	9.7	-24	1993/2/5	42	1
	HD100764	9.0	+5	1993/2/2,3	87	2
	BD+42°2173	10.44	-76	1995/3/18	71	1
	HD187216	9.57	-129	1994/8/7	96	1
4700 Å$\sim$ 4760 Å	HD112869 (TT CVn)	9.16	-135	1995/3/20	39	1
	HD201626	8.14	-152	1995/8/21	46	1
	HD26	8.25	-213	1995/8/26	63	1
	HD13826 (V Ari)	8.3	-176	1995/8/26	51	1
	HD5223[b]	8.48	-232	1968/10/11	-	1

[a] References: (1) Hartwick et al. (1985), (2) Keenan (1993) and Dominy (1984)
[b] Based on photographic plate.

Table 2. Molecular data

line positions	
CN red system	^{12}CN:Davis and Philips (1963)
	^{13}CN:Wyller (1966)
C_2 Swan system	$^{12}C_2$:Philips and Davis (1968)
	$^{12}C^{13}C$:Pesic et al. (1983)
rotational constants	
CN red system	Huber and Herzberg (1979)
C_2 Swan system	Amiot (1983)
band oscillator strengths	
CN red system	Bauschlicher et al. (1988)
C_2 Swan system	Naulin (1988)
Hőnl-London factors	
CN red system	Earls (1935), Schadee (1967)
C_2 Swan system	Danylewych et al. (1974)

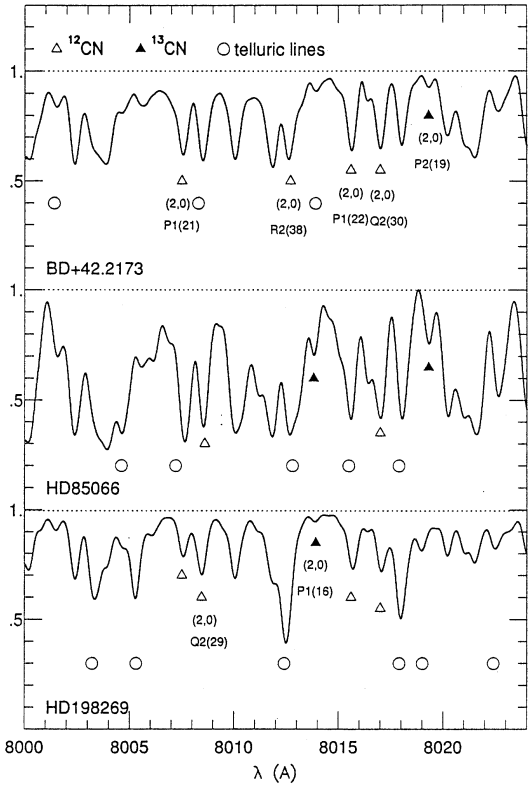

Fig. 1. Examples of spectra in the near infrared region. Telluric lines affect them at the wavelengths marked by open circles. Open and filled triangles mean lines of ^{12}CN and ^{13}CN, respectively.

one of good probes of stellar evolution. Generally the $^{12}C/^{13}C$ ratio and total carbon abundance decrease due to the convection which dredges up the products of internal CNO cycle to stellar atmosphere as ascending RGB. After that, if it reaches AGB stage, the fresh ^{12}C may be supplied from the internal He burning layer to stellar surface and the star may become a carbon star, and $^{12}C/^{13}C$ ratio increases again. Is this model valid to metal-poor carbon stars? Tsuji et al. (1991) has shown that there should be two kinds of CH stars; one with very high $^{12}C/^{13}C$ ratio and the other with the values about 10. We observed further objects and report the results in this paper.

2. Observations and measurements

The sample of this program is selected from the list of Hartwick & Cowley (1985) except for HD100764 which is classified as CH star by Keenan (1993). As shown in Table 1 most of these stars are high velocity stars, except for HD85066 and HD100764.

Observations are done by the coudé spectrograph of the 1.88m reflector at Okayama Astrophysical Observatory (OAO[1]). We used 640×1024 RCA CCD detector with pixel size of 15×15 μm. For CN red system ($A^2\Pi - X^2\Sigma$), we have observed the spectral region from 7790 Å to 8030 Å by two exposures. We used F/10 camera with 1200 grooves/mm grating, and the dispersion is 8 Å/mm at 8000 Å. The resolution is about 0.4 Å, which is derived from the FWHM of weak comparison lines (thorium). Also, for C_2 Swan system ($A^3\Pi_g - X^3\Pi_u$), we have observed the spectral region from 4700 Å to 4760 Å. The dispersion is 4 Å/mm at 4700 Å and the resolution is about 0.21 Å.

We have done normal reduction which includes dark subtraction, flat fielding and wavelength calibration. Examples of the spectra in the red region for three stars are shown in Fig. 1, and details of the observations are given in Table 1. We observed early type stars (α Lyr or α Leo) to obtain the spectra of telluric lines, which are rich in the near infrared region. We excluded the CN lines which may be affected by telluric lines from our analysis.

One spectrogram of HD5223 by the photographic plate was also used. This observation was done by the coudé spectrograph of the 2.5m Hooker telescope at Mt. Wilson Observatory nearly 30 years ago. By the use of the f = 0.8 m camera with IIaO plate, a well exposed spectrogram of the dispersion of about 4.3 Å/mm was obtained by an exposure time as long as 400 min. The spectrogram was digitized by the PDS microdensitometor of our institute and reduced to the intensity scale by the use of the calibration wedge spectra.

Because CH stars do not show so strong absorption as cool carbon stars, their continuum levels can be determined reasonably well by the interpolation of the levels in the wavelength region free from strong CN molecular absorption. Equivalent widths of CN lines are measured by assuming the profile to be Gaussian. For the stars whose molecular lines are strong (HD224959, HD187216 and HD85066), however, we could not measure the FWHM of CN lines and assumed it to be a typical value 0.5 Å. As the FWHMs of the spectral lines are determined mostly by the instrumental profile rather than by the intrinsic stellar line profile at the resolution (about 15 km/sec) we have employed, the equivalent widths are essentially determined by the observed line depths. An advantage to transform the central depth to the equivalent width is simply that we can apply the classical theory of the curve-of-growth to the equivalent widths but not to the central depths.

3. Atmospheres of CH stars

3.1. Effective temperatures

Effective temperatures ($T_{\rm eff}$'s) of 6 stars (TT CVn, V Ari, HD26, HD201626, HD224959 and HD198269) are determined by means of the infrared flux method (IRFM, Blackwell et al. 1980). The IRFM uses the ratio of bolometric flux which is proportional to $T_{\rm eff}^4$ to an infrared flux which is relatively free from strong absorption and hence roughly proportional to $T_{\rm eff}$, e.g. L-band flux. $T_{\rm eff}$ can be determined once the relation between this ratio and $T_{\rm eff}$ can be calibrated by the model atmospheres described in the next section. The fluxes can be obtained by the transformation from photometric data based on the absolute calibration of each photometric system. The photometric data derived by Dominy et al. (1986), Eggen (1972a), Feast et al. (1992) and Gezari et al. (1993) are used. The transformation to absolute infrared flux is based on the spectral energy distribution (SED) of α Lyr calibrated by Blackwell et al. (1983). We adopted L-band flux for the infrared flux and calculated the ratio ($R_{\rm L}$) of bolometric flux to the L-band flux. We use model atmospheres whose metallicity (Z) is 1/10 of the solar ($\log Z/Z_\odot = -1$) to calibrate the relation between $R_{\rm L}$ and $T_{\rm eff}$. The $T_{\rm eff}$'s determined by the IRFM depend only weakly on metallicity. Varying the $\log Z/Z_\odot$ of the model atmosphere by 1.0 dex changes the $T_{\rm eff}$ by only $50 \sim 100$ K.

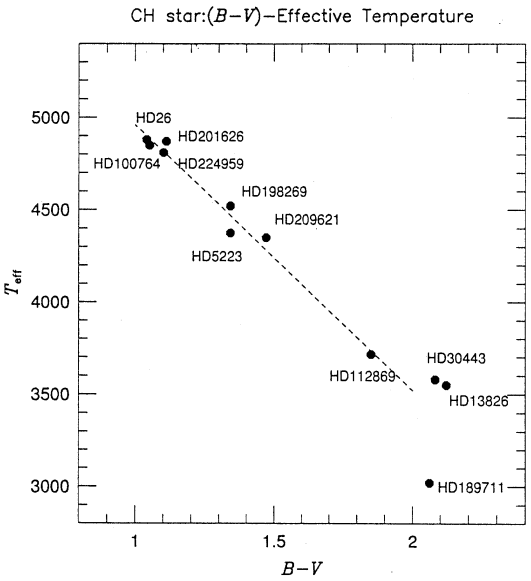

Fig. 2. Correlation between effective temperatures and $B-V$ colors for CH stars. Effective temperatures of 11 stars shown by filled circles in this figure are determined by means of the infrared flux method, except for HD100764 which is derived from $V-R$ color by Dominy (1984). The solid line is fitted to 8 stars with $B-V$ smaller than 2. We used this relation to estimate $T_{\rm eff}$'s of BD+42°2173, HD187216 and HD85066.

For HD100764 $T_{\rm eff}$ = 4850 K derived by Dominy (1984) is used.

We could not use the IRFM for BD+42°2173, HD187216 and HD85066 since photometric data necessary to calculate the bolometric flux are not available. For these stars a relation of $T_{\rm eff}$ with $B-V$ in CH stars is used. This relation is shown in Fig. 2, where $T_{\rm eff}$ of each CH star is mainly determined by the IRFM. The relation is nearly linear in the region of $1.0 \leq B-V \leq 2.0$. $(B-V)$'s of these stars are given in Table 3.

[1] OAO is a branch of National Astronomical Observatory of Japan (NAOJ). This work was carried out under the common use program of OAO.

Table 3. Effective temperatures

Star Name	$B-V$	$f_{\rm bol}^{\rm a}$(erg/sec/cm^2)	$f_{\rm L}^{\rm b}$(erg/sec/cm^2/cm)	$T_{\rm eff}$ (K)
HD224959	1.10	4.902×10^{-9}	9.836×10^{-7}	4800
HD198269	1.34	2.435×10^{-8}	5.927×10^{-6}	4520
HD85066	1.75	-	-	3900
HD100764	1.05	-	-	4850
BD+42°2173	1.34	-	-	4500
HD187216	1.69	-	-	4000
TT CVn	1.85	2.009×10^{-8}	8.690×10^{-6}	3715
HD201626	1.11	2.239×10^{-8}	4.325×10^{-6}	4870
HD26	1.04	1.722×10^{-8}	3.304×10^{-6}	4880
V Ari	2.12	6.209×10^{-8}	2.999×10^{-5}	3580

[a] $f_{\rm bol}$: observed bolometric flux. Photometric data are based on Dominy et al. (1986), Eggen (1972a), Feast et al. (1992) and Gezari et al. (1993)
[b] $f_{\rm L}$:observed flux at the L band.

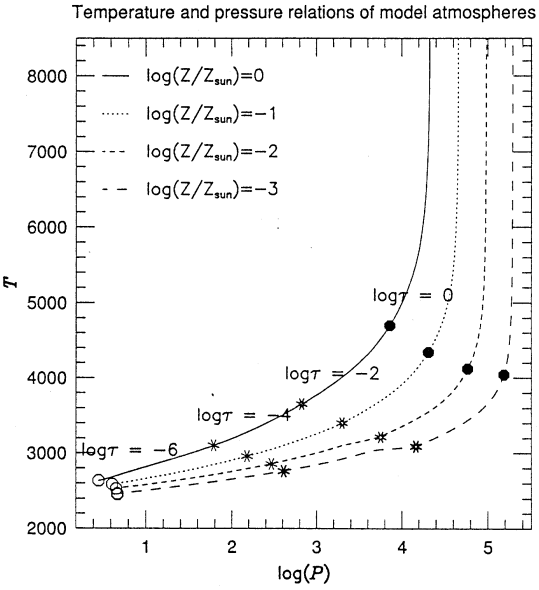

Fig. 3. Temperature and pressure relations of model atmosphere for 4 cases of metallicity ($T_{\rm eff}$ = 3900 K, log$g$ = 2.0, $\xi_{\rm micro}$ = 3.0 km/s).

3.2. Model atmospheres

Model atmospheres are calculated for several cases of metallicities and for effective temperatures between 3300 and 5100K. In the calculation we assumed plane-parallel and homogeneous atmospheres in radiative equilibrium. Also hydrostatic equilibrium, including radiation and turbulent pressures, is assumed in the 80 layers between log $\tau_0 = -6.0$ and +1.9 (τ_0 means the continuum optical depth at 1.04 μm). LTE is assumed in evaluation of the molecular abundances and opacities. Opacities from the usual continuous absorption sources and the line absorption of molecules CO, CN, C_2, HCN and C_2H_2 are considered. We applied the band model method for the molecular line opacities and the spectral region between 0.2 and 50 μm is divided into 194 spectral meshes which are further divided into 5 submeshes.

The pressure-temperature structures of model atmospheres with log $Z/Z_\odot = 0, -1, -2$ and -3 (log $T_{\rm eff}$ = 3900 K, log g = 2.0 and C/O = 3, throughout) are shown in Fig. 3, where the depths corresponding to log $\tau_0 = 0, -2, -4$ and -6 are indicated by different symbols. It is obvious that the pressure is higher in the metal-poor atmosphere than in metal-rich one at the given point of log τ_0.

As a test of our model atmospheres, the predicted SEDs are compared with the observed ones for HD26 and TT CVn in Fig. 4. For HD26 three SEDs based on model atmospheres with $T_{\rm eff}$ = 5100 K, 4800 K and 4500 K are shown (log g = 2.0 and log $Z/Z_\odot = -1$, throughout). We find that the observed SED can be reproduced well by the model atmosphere with $T_{\rm eff}$ = 4800 K. This is consistent with the $T_{\rm eff}$ determined by the IRFM which is almost independent of metallicity (see Sect. 3.1). Then the model atmosphere of HD26 is reasonable one even though several assumptions for model parameters are included.

Next, for TT CVn, we assume that $T_{\rm eff}$ is well determined by the IRFM and discuss the effects of metallicity on model atmospheres and their SEDs. Three SEDs based on model atmospheres with log $Z/Z_\odot = -1, -2$ and -3 are shown in Fig. 4 ($T_{\rm eff}$ = 3700 K and log g = 0.0, throughout). We find that the L-band flux is almost independent of metallicity and confirmed the advantage of determining $T_{\rm eff}$ by the IRFM. On the other hand we find stronger depression in optical ($\lambda \leq 1.0\mu$m) region in more metal-poor atmosphere. This tendency is contrary to the well-known UV-excess by line deblanketing in metal-poor stars although atomic line blanketing effect is not included in our model atmospheres. However, this effect is also seen in the region free from strong atomic lines. In cool stars such as TT CVn, this can be understood as the result of the stronger Raileigh scattering by neutral hydrogen relative to absorption by H^- ion in more metal-poor stars. Then, since $T_{\rm eff}$ is determined well by the IRFM, metallicity can be roughly presumed by the comparison of observed SED with predicted one. We find that log $Z/Z_\odot$ may be between -2.0 and -1.0 for TT CVn, but cannot be so low as -2.9 suggested by Kipper (1992).

3.3. Line intensities

The formation of C_2 and CN will be more reduced than that of CH in metal-poor atmosphere as compared with that in the metal-rich one because the abundances of carbon and nitrogen are low in the metal-poor stars while hydrogen abundance is expected not to vary in stars. This results in relatively strong CH band in metal-poor carbon star. Further, as shown in Fig. 3, the high pressure of metal-poor atmosphere results in easier molecular formation. Then CH band in metal-poor carbon stars can be even stronger than in metal-rich carbon stars.

We calculate theoretical line intensities (Γ's) for CH and C_2, and show them in Fig. 5. Γ is obtained by integration of molecular density with weighting function based on model atmosphere (Cayrel & Jugaku 1963). Note that log W/λ is equal to log gf + log Γ in the weak line limit (here W and λ mean

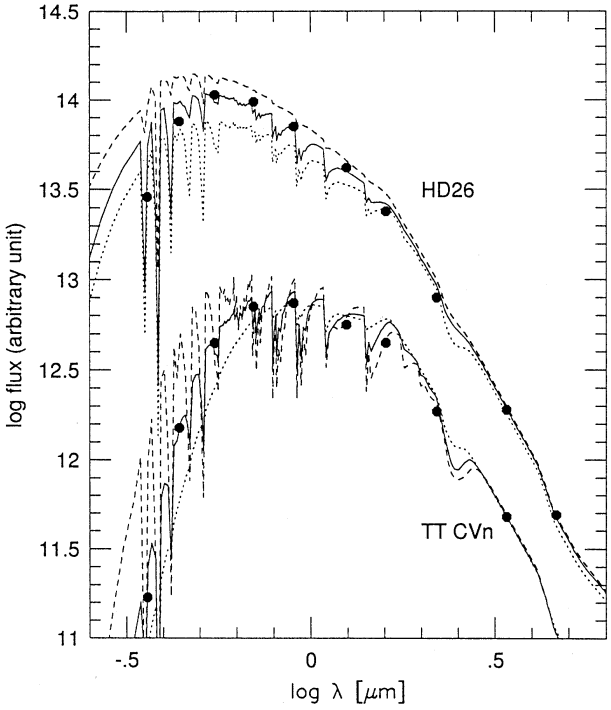

Fig. 4. The observed spectral energy distributions (SEDs) of two CH stars based on the photometry are shown by the filled circles. These observed SEDs are compared with the predicted SEDs based on model atmospheres for which the parameters are as follows; For HD26 three cases of $T_{\rm eff}$ = 5100 K (dashed line), 4800K (solid line) and 4500K (dotted line) with log g = 2.0, log $Z/Z_{\odot} = -1$ and $\xi_{\rm micro}$ = 3 km/s. For TT CVn log $Z/Z_{\odot} = -1$ (dashed line), log $Z/Z_{\odot} = -2$ (solid line) and log $Z/Z_{\odot} = -3$ (dotted line) with $T_{\rm eff}$ = 3700 K, log g = 0.0 and $\xi_{\rm micro}$ = 3 km/s.

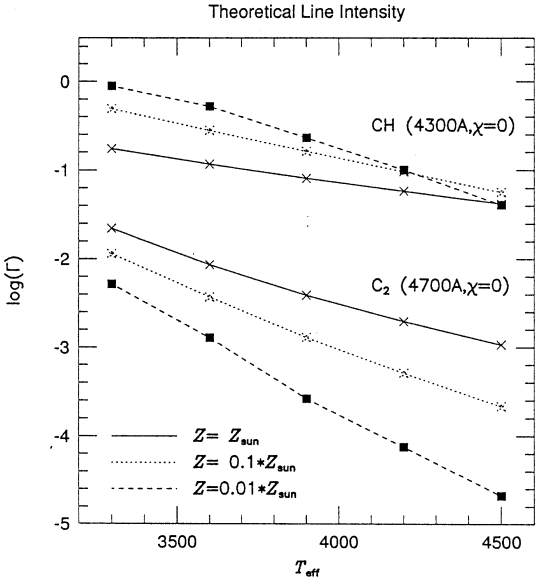

Fig. 5. Theoretical line intensities (Γ's) based on model atmospheres for various metallicities. The intensities are calculated for λ = 4300 Å, χ = 0 eV for CH and λ = 4700 Å, χ = 0 eV for C_2. Larger Γ means stronger line.

equivalent width and wavelength of the line, respectively). As shown in Fig. 5, Γ for CH (4300 Å) is larger while Γ for C_2 (4700 Å) is clearly smaller in metal poor model atmospheres than in metal-rich models.

4. Analysis and results

4.1. Curve-of-growth analysis on CN red system

For the calculation of the line list of CN red system we used molecular data shown in Table 2. We adopted the value of 7.66 eV as the dissociation energy of CN molecule. The uncertainty of the dissociation energy is large, but that cancels out in deriving the isotope ratio. With the measured equivalent widths (W's) of ^{12}CN and ^{13}CN lines, we plot log W/λ against log X = log gf + log Γ, where Γ means the theoretical line intensity based on model atmospheres (see Sect. 3.3). They are shown in Fig. 6, where ^{12}CN and ^{13}CN lines are plotted by the open and filled circles, respectively. The weakest lines of ^{12}CN are comparable with ^{13}CN lines in intensity. Thus, the horizontal shift between the curve-of-growth for ^{12}CN and that for ^{13}CN is a direct measure of ^{12}C/^{13}C ratio (the iso-intensity method). Results by this method are shown in Table 4, where the resulting ^{12}C/^{13}C ratios distribute between 4 and 15.

All of the lines plotted in Fig. 6 are those from (2,0) band, and the lower excitation potentials of the ^{13}CN lines differ from those of ^{12}CN lines of the comparable strengths by only 0.25 eV. If the uncertainty of temperature structure of model atmosphere, which may also be due to uncertainty of $T_{\rm eff}$ or of other parameters, is assumed to be $\Delta T = \pm 250$ K at T = 4250 K ($\Delta\theta \simeq 0.07, \theta = 5040/T$), uncertainty of the horizontal shift is $\Delta \log \Gamma \simeq \chi \Delta\theta \simeq 0.017$, which affects the uncertainty of ^{12}C/^{13}C ratio by only 4%. Thus, an uncertainty of models results in a minor error in the ^{12}C/^{13}C ratio so far as the iso-intensity method can be applied directly.

We determined the micro-turbulent velocity ($\xi_{\rm micro}$) by fitting the theoretical curves-of-growth based on model atmospheres to the observed one of ^{12}CN lines. The resulting ^{12}C/^{13}C ratios by the iso-intensity method do not depend on the theoretical curve-of-growth nor on the micro-turbulent velocity we adopted, but we derived $\xi_{\rm micro}$ for a check of the consistency of these curves-of-growth. The derived micro-turbulent velocities are between 2 and 3 km/s as given in Table 4. These values are normally expected for red giants.

Systematic (external) errors by uncertainty of model atmosphere and its parameters are quite small in the results by the iso-intensity method as outlined above. Therefore errors in ^{12}C/^{13}C ratio mainly depend on internal errors in measurements of equivalent widths, which depend on the continuum levels adopted as well as on measurements of FWHMs and depths of the absorption lines. The errors in measurements result in the errors of the ^{12}C/^{13}C ratios smaller than 50 % for BD+42°2173, HD224959 and HD198269 for which weak lines can be used, while some-

Table 4. Results by CN red system

Star	$T_{\rm eff}$ (K)	$\xi_{\rm micro}$(km/sec)	^{12}C/^{13}C
HD224959	4800	2	7
HD198269	4500	3	7
HD85066	4200	3	11
HD100764	4800	3	4
BD+42°2173	4500	3	15
HD187216	4000	3	10

what larger for HD85066, HD187216 and HD100764 but the errors are still smaller than factor 2.

4.2. Spectral synthesis on C_2 Swan band

Previously, the lower limits of ^{12}C/^{13}C about 200 and 680 have been derived for TT CVn and V Ari, respectively, by the analysis of CN red system (Tsuji et al. 1991), because ^{13}CN lines were too weak to compare their equivalent widths with those of ^{12}CN. Also HD26 and HD201626 show so weak CN lines that we cannot measure precisely the equivalent widths of ^{13}CN lines. For this reason we tried to determine the ratio for these stars by an analysis of the stronger C_2 Swan band in the present work.

We calculate the synthetic spectra of C_2 Swan system based on our model atmospheres. We used molecular data shown in Table 2 to calculate the line list of C_2 Swan system. The band oscillator strength we use is $f_{10} = 12.7\times10^{-3}$, which is obtained by the measurement of lifetime τ = 97 ns (Naulin 1988).

As a test, we first tried to fit the synthetic spectra based on this molecular line list to the spectrum of HD5223, for which ^{12}C/^{13}C ratio is well determined from the curve-of-growth analysis of CN lines. We adopt $T_{\rm eff}$ = 4500 K, log$g$ = 2.0, $\log Z/Z_\odot = -1$ and $\xi_{\rm micro}$ = 3 km/s as the model parameters (Tsuji et al. 1991). The synthetic spectra are convolved with the instrumental profile, for which we use the Gaussian of FWHM = 15 km/s throughout this analysis. We show the results in Fig. 7, where the observed and synthetic spectra are shown by the dots and the lines, respectively. For the calculation of synthetic spectra we used mainly the atomic line data of Meggers et al. (1975) for heavy elements and of Fuhr et al. (1988) for iron, respectively. For the region around 4744 Å, i.e. around the band head of ^{12}C^{13}C, we used the line list of Kurucz & Bell (1995) for other elements. Because we cannot determine the abundances of heavy elements as well as of iron accurately in this work, we must consider the uncertainties of these abundances in the following analyses. We mainly fit the synthetic spectra to the observed feature of $^{12}C_2$ band in the region around 4735 Å because atomic lines are relatively weak in the wavelength region between 4734 Å and 4736 Å, while there is a strong iron line in the region with the strongest absorption around 4737 Å. We found ^{12}C/^{13}C $\simeq$ 10, which agrees well with the previous results based on a more empirical iso-intensity method for individual lines of CN (^{12}C/^{13}C = 9, Tsuji et al. 1991). By this analysis of HD5223 we conclude that the method of spectral synthesis on C_2 Swan band is useful to determine ^{12}C/^{13}C ratios even if the uncertainty is lager than that of the iso-intensity method.

Table 5. Results by C_2 Swan system for HD201626 and HD26

	$T_{\rm eff}$ (K)	log g	$\log Z/Z_\odot$	$\xi_{\rm micro}$ (km/s)	^{12}C/^{13}C
HD201626	4800	2.0	−1.5	2.0	40
HD26	4800	2.0	−0.5	2.0	10

In the calculations of the synthetic spectra we adopted $\xi_{\rm micro}$ = 2 km/s and $\log Z/Z_\odot = -0.5$ for HD26 and also $\xi_{\rm micro}$ = 2 km/s and $\log Z/Z_\odot = -1.5$ for HD201626. These values are based on $\xi_{\rm micro}$'s and iron abundances derived by Vanture (1992a) which are roughly consistent with those of Wallerstein & Greenstein (1964). The spectra are shown in Figs. 8a and b. The wavelength region fitting the synthetic spectra to observed one is the same as the case of HD5223. We find in Figs. 8a and b that the continuum can be well determined using the region to the red of 4740 Å. The results are ^{12}C/^{13}C $\simeq$ 10 and 40 for HD26 and HD201626, respectively (Table 5). As shown in Figs. 8a and b, if we assume that the ^{12}C/^{13}C ratios are larger and smaller by a factor of 2 than ^{12}C/^{13}C = 10 and 40 for HD26 and HD201626, respectively, the synthetic spectra obviously do not fit the observed spectra.

Although there is no preferable line in our spectra to determine iron abundances accurately, we can fit the synthetic spectra to the observed spectra when we assume smaller iron abundances to calculate synthetic spectra than those of Vanture (1992a). One of the reasons will be that we adopt lower $T_{\rm eff}$'s by 300 or 400 K for these two stars than those of Vanture (1992a). Also we fit the synthetic spectra to observed spectra for lines of heavy elements such as Zr, La, Ce etc. as shown in Figs. 8a and b. The abundances of these elements which we use to calculate the synthetic spectra are systematically larger by about 0.4 dex than those derived by Vanture (1992c). Since the uncertainty of iron and heavy elements abundances noted above should be considered, the metallicities are varied by a factor of three, and we find that the resulting ^{12}C/^{13}C ratios differ by less than 50% for both HD26 and HD201626. Also ^{12}C/^{13}C ratios of HD201626 are determined by assuming $\xi_{\rm micro}$ = 1 km/s and 3 km/s, and the resulting ^{12}C/^{13}C ratios differ by less than 50%. We conclude that the errors of ^{12}C/^{13}C ratios are less than a factor of 2 for HD26 and HD201626.

The observed spectrum of TT CVn is shown in Fig. 9a. The $^{12}C_2$ band is strongly saturated and the synthetic spectra depend severely on parameters of model atmosphere. On the other hand, model parameters of TT CVn are not determined so accurately, especially for micro-turbulent velocity and metallisity. Therefore only a lower limit of carbon isotope ratio is determined based on the following considerations. First, strong absorption lines in synthetic spectra are significantly influenced by $\xi_{\rm micro}$. While ^{12}C^{13}C band is weak and not sensitive to $\xi_{\rm micro}$, the absorption of $^{12}C_2$ is stronger for larger $\xi_{\rm micro}$, therefore ^{12}C/^{13}C is smaller for larger $\xi_{\rm micro}$. A value of $\xi_{\rm micro}$ = 6 km/s has been

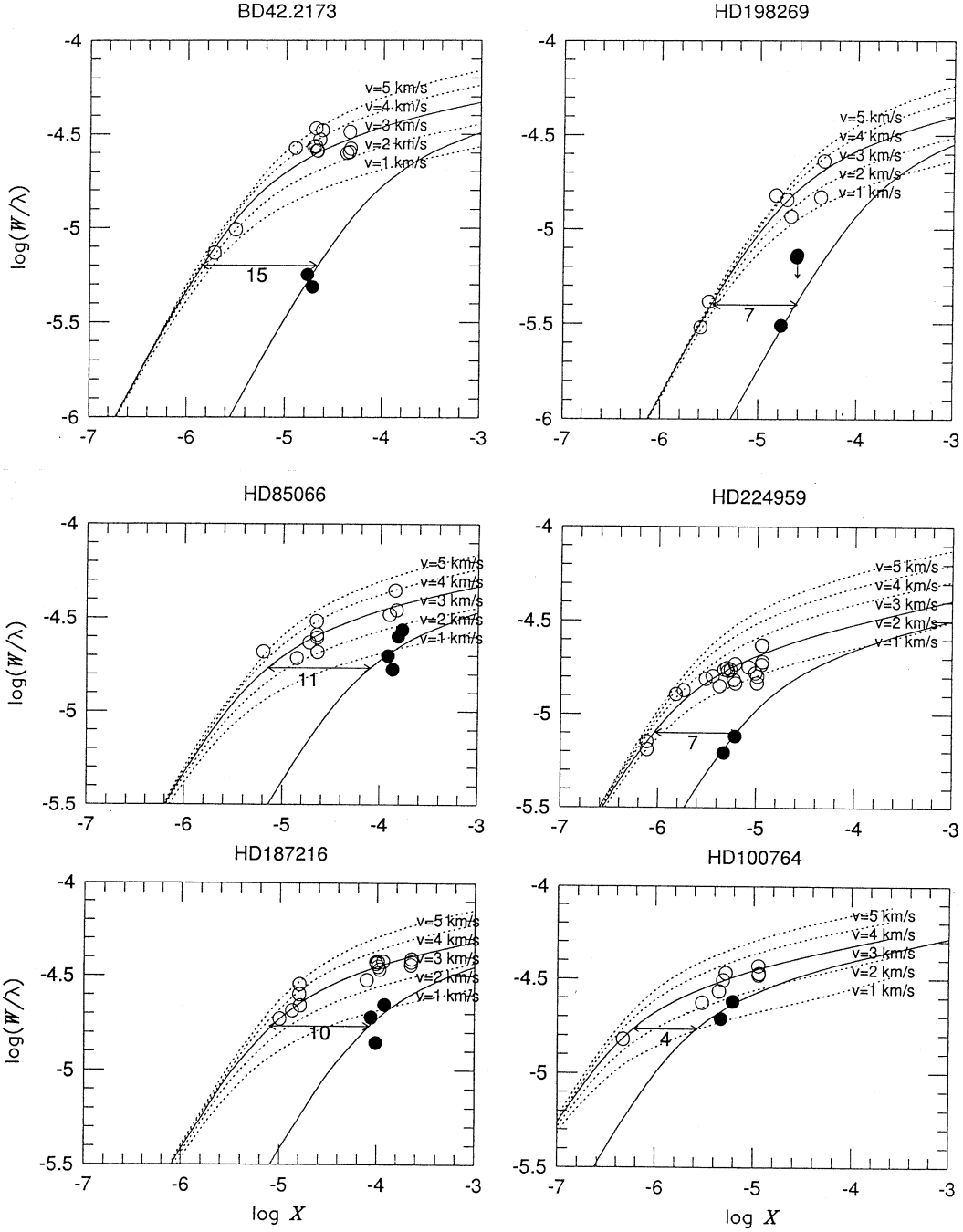

Fig. 6. The curves-of-growth for ^{12}CN (open circles) and ^{13}CN (filled circles). Theoretical curves-of-growth for ^{12}CN lines are shown for the turbulent velocities 1, 2, 3, 4 and 5 km/sec. The line which fits best to each empirical one is shown by the solid line and adopted to determine the turbulent velocity. The arrow in the curve-of-growth for HD198269 implies that the equivalent width is upper limit.

derived by the analysis of ^{12}CN lines (Tsuji et al. 1991) which is extremely large as compared with those in other CH stars ($\simeq$ 3 km/s). We adopted 6 km/s to determine the lower limit of ^{12}C/^{13}C ratio. Second, the ^{12}C/O ratio is determined for each case by fitting the calculated feature of $^{12}C_2$ band to observed one. $^{12}C_2$ band is not so sensitive to ^{12}C/O ratio because most of the lines are saturated. We adopted the smallest ^{12}C/O ratio by which we could fit the spectrum, because smallest ^{12}C abundance give the lowest ^{12}C/^{13}C ratio. In the above two conditions, some cases of chemical composition, effective temperature and gravity are tried. The spectral feature of TT CVn is different from those of HD26 and HD201626. In this case the fitting of synthetic spectrum to observed one is not good as shown in Fig. 9a and, then, there are probably unidentified lines around 4744 Å. However it will be able to determine the lower limit of ^{12}C/^{13}C ratio. The results are summarized in Table 6 with

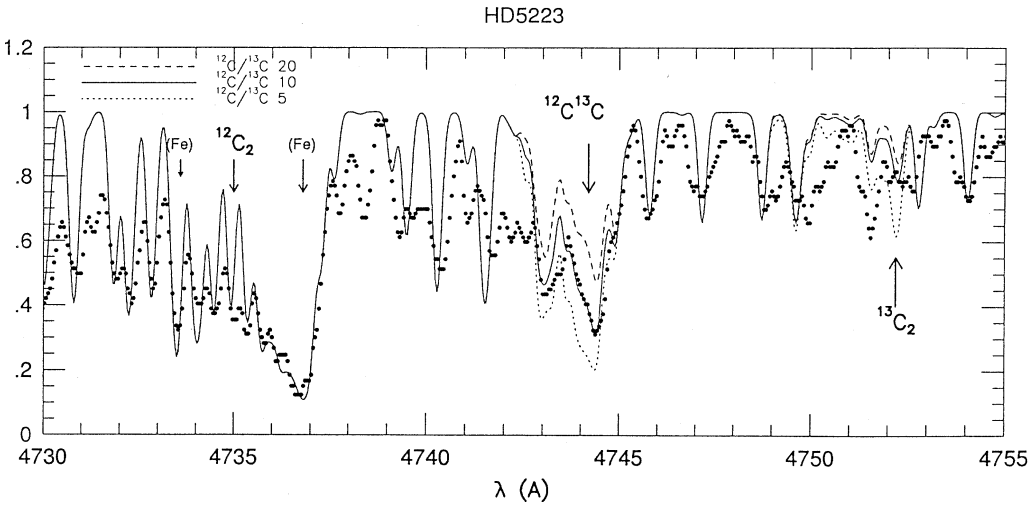

Fig. 7. The observed spectrum of HD5223 is shown by dots, and synthetic spectra for $^{12}C/^{13}C = 5$, 10, and 20 based on the model atmosphere ($T_{\rm eff}$ = 4500 K, $\log g$ = 2.0, $\log Z/Z_\odot = -1$ and $\xi_{\rm micro} = 3$ km/s) are shown by the dotted, solid and dashed lines, respectively. The carbon abundance is estimated to be C/O = 3.0 and $^{12}C/^{13}C$ ratio is about 10. We confirmed that this method and the list of lines are useful for determination of the carbon isotope ratio.

Table 6. Results by C_2 swan system for TT CVn and V Ari

	$T_{\rm eff}$ (K)	$\log g$	$\log Z/Z_\odot$	$\xi_{\rm micro}$ (km/s)	$^{12}C/^{13}C$	C/O
TT CVn	3700	2.0	−2.0	3.0	> 5000	10
	3700	2.0	−2.0	6.0	> 500	3.4
	3900	2.0	−2.0	6.0	≥ 500	5.0
	3700	0.0	−2.0	6.0	≥ 500	6.3
	3700	2.0	−1.0	6.0	> 500	2.1
	3700	0.0	−3.0[a]	6.0	≥ 1000	20
V Ari	3600	2.0	-1.0	6.0	≥ 100:	2

[a] [O/Fe] = +0.5

parameters assumed. In the first line of the Table 6 we show the case where the micro-turbulent velocity is assumed to be 3 km/s as a reference. The resulting $^{12}C/^{13}C$ ratio is as high as 5000 and this case clearly does not give the lower limit of $^{12}C/^{13}C$ ratio. The lower limit of $^{12}C/^{13}C$ of about 500 has been derived from the cases where micro-turbulent velocities are assumed to be 6 km/s.

The spectrum of V Ari is shown in Fig. 9b. The lines are too strong to determine the continuum level, and accordingly to derive accurate carbon isotope ratio. For this star the result that the lower limit of $^{12}C/^{13}C$ is 680 and micro-turbulent velocity is 6 km/s has been derived by the analysis of CN lines in Tsuji et al. (1991). If we adopt this micro-turbulent velocity and try to analyse by the same method as TT CVn, the isotope ratio is about 100 or larger. This result is, of course, very uncertain but not inconsistent with the previous result that this star has extremely high $^{12}C/^{13}C$ ratio.

4.3. Comparisons with other authors

For some of the stars analysed in this work, the $^{12}C/^{13}C$ ratios have been derived by other authors. Their results are compared with ours in Table 7. We agree rather well with Kipper & Jørgensen (1994) for HD187216 and with Vanture (1992a) for HD198269. However, we do not agree in other cases as follows.

Vanture (1992a) has shown the $^{12}C/^{13}C$ ratio to be 3 for HD224959 by the spectral synthesis method for C_2 Swan band and to be 13 by the same method for CN red system at the same time. One of his results is by two times larger and the other is smaller by the same factor than our result of $^{12}C/^{13}C$ = 7 based on the iso-intensity method. The error of our result is smaller than 50% as noted in Sect. 4.1. On the other hand Vanture (1992a) pointed out that the large discrepancy in his results may be explained as the result of the saturation of ^{12}CN lines. Vanture's explanation is that ^{12}CN lines are more sensitive to the uncertainties of micro-turbulent velocity than C_2 lines because the equivalent widths of individual ^{12}CN lines are greater than 100 mÅ while those of $^{12}C_2$ lines are less than 60 mÅ. But the strength of lines should be represented by W/λ rather than by W itself. The wavelength region of CN lines is greater than that of C_2 lines by factor 1.7. Therefore W/λ of CN line with W=100 mÅ is nearly the same as W/λ of C_2 line with W=60 mÅ. Then the effect of saturation in ^{12}CN lines would not explain the discrepancy in his result. Vanture's result may reveal a difficulty of the spectral synthesis method which sometimes produces the results that differ by factor of 4 or more for different spectral features of the same star. Clearly the iso-intensity method is preferred if intensities of individual lines can be measured.

For both HD26 and HD201626, Vanture (1992a) derived $^{12}C/^{13}C \geq 25$. Our result of about 10 for HD26 is smaller at least by a factor of 2, while our result of 40 for HD201626 may

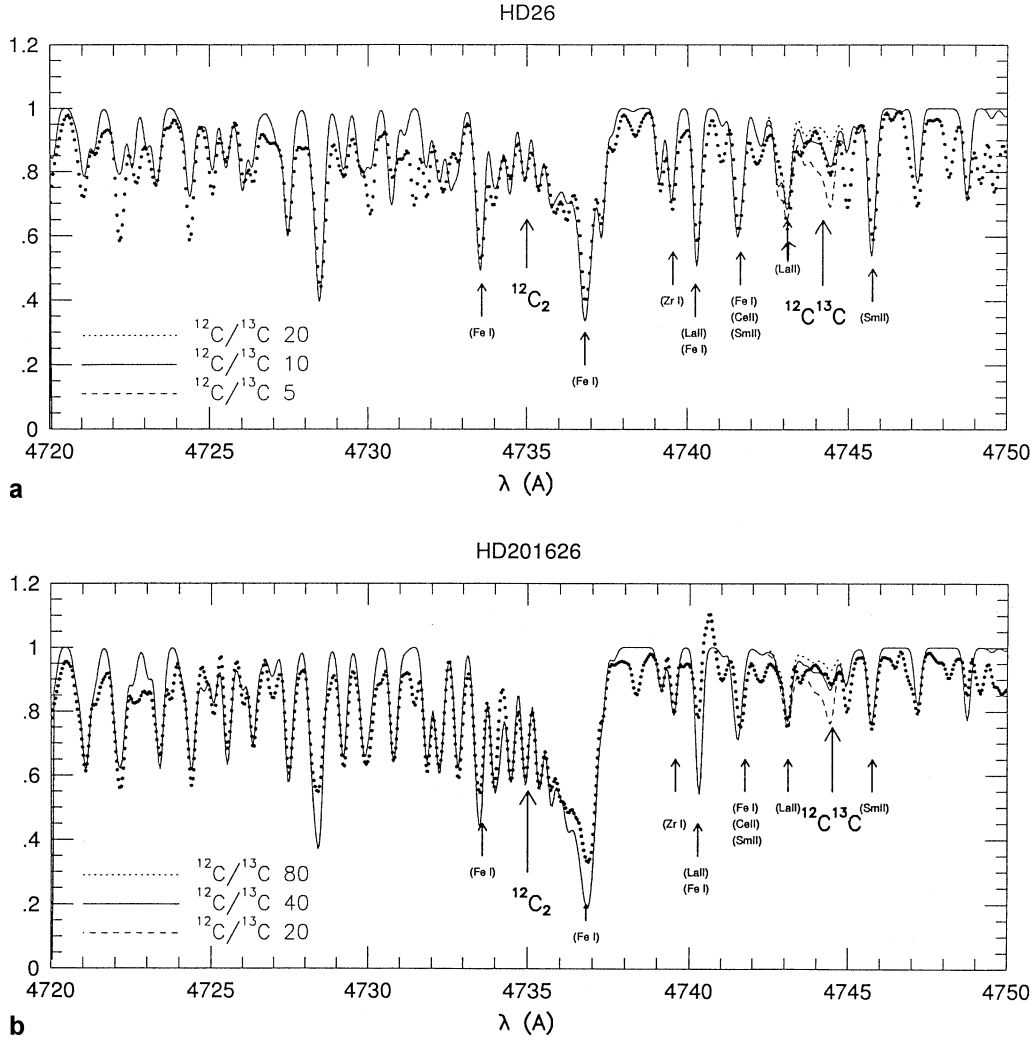

Fig. 8. a The observed spectrum of HD26 and the synthetic spectra based on the model atmosphere ($T_{\rm eff}$ =4800 K, log g = 2.0, log $Z/Z_{\odot} = -0.5$ and $\xi_{\rm micro}$ = 2 km/s). The carbon abundance is estimated to be C/O = 1.4. We determine ^{12}C/^{13}C ratio to be about 10 for this star. **b** The observed spectrum of HD201626 and the synthetic spectra based on the model atmosphere ($T_{\rm eff}$ = 4800 K, log g= 2.0, log $Z/Z_{\odot} = -1.5$ and $\xi_{\rm micro}$ =2 km/s). The carbon abundance is estimated to be C/O = 2.2. We determine ^{12}C/^{13}C to be about 40 for this star.

be larger by about a factor of 2 than the result of Vanture. The observed spectrum of HD26 clearly show weaker $^{12}C_2$ band and stronger $^{12}C^{13}C$ band than that of HD201626 (see Figs. 8a and b). Hence our result that the ^{12}C/^{13}C ratio of HD26 is at least smaller than that of HD201626 should be correct. In this case, we also applied the spectral synthesis method which is not always reliable as we just see above, but it can at least discriminate the difference of ^{12}C/^{13}C ratios if the observed band strengths are so different as in the case of HD26 and HD201626. Effective temperature adopted in our analysis for both HD26 and HD201626 is 4800 K which is lower than that in Vanture by about 300 $\sim$ 400 K. But we calculated synthetic spectra based on the model atmosphere with $T_{\rm eff}$ = 5100 K and confirmed that this difference of effective temperature cannot influence the isotope ratio so much.

The chemical composition of TT CVn was derived by Kipper (1992) who gave [Fe/H] = -2.9, C/O = 1.07 and ^{12}C/^{13}C = 50 $\sim$ 90. The carbon isotope ratio differs largely from our result (^{12}C/^{13}C $\geq$ 500 or, at least, $\geq$ 200) which is based on two independent analysis. We think that his fixed oxygen abundance log $A_{\rm O} = -3.20$ (i.e. solar level) will be too large for the metallicity he derived (log $A_{\rm Fe} = -7.3$). We suspect that this unrealistic assumption might result in C/O ratio as small as 1.07 while we suggest that C/O ratio may be rather large (2.1$\sim$10) for this star (Table 6).

5. Discussion

5.1. Distribution of $^{12}C/^{13}C$ ratio in carbon stars of the Galactic halo

From results shown in Tables 4 $\sim$ 6 and Tsuji et al. (1991), both are based on observations at OAO, we obtain the distribution of carbon isotope ratio shown in Fig. 10. Though no star with very

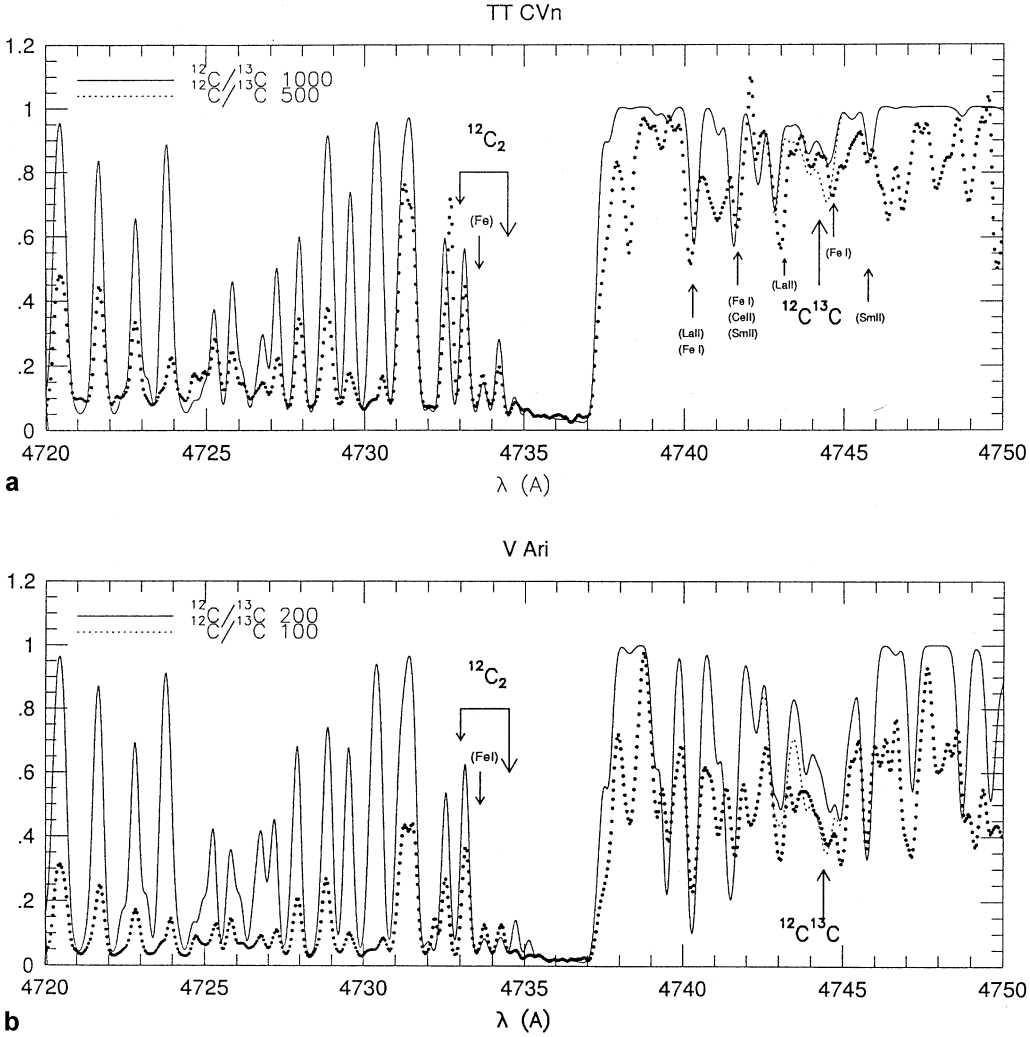

Fig. 9. a The observed spectrum of TT CVn and the synthetic spectra based on the model atmosphere ($T_{\rm eff}$ = 3700 K, log g = 2.0, log $Z/Z_\odot = -2.0$ and $\xi_{\rm micro}$ = 6 km/s). The carbon abundance is estimated to be C/O = 3.4. Several lines are not reproduced in synthetic spectra as seen in the region to the red of 4740 Å and probably there will be unidentified lines in the wavelength region of $^{12}C^{13}C$ band. By this reason we can only determine the lower limit of $^{12}C/^{13}C$ ratio. This is one of the cases to derive the lower limit of $^{12}C/^{13}C$ ratio for this star. In this case we find that $^{12}C/^{13}C$ ratio is larger than 500. **b** The observed spectrum of V Ari and the synthetic spectra based on the model atmosphere ($T_{\rm eff}$ = 3600 K, log g = 2.0, log $Z/Z_\odot = -1.0$ and $\xi_{\rm micro}$ = 6 km/s). The carbon abundance is estimated to be C/O = 2. In this case the accurate determination of $^{12}C/^{13}C$ is very difficult because the continuum level cannot be determined clearly and the $^{12}C_2$ band is so heavily saturated.

high $^{12}C/^{13}C$ ratio such as V Ari and TT CVn is found in the present survey, more severe lower limit has been derived for TT CVn. Our result suggests that CH stars can be divided into two groups; one with $^{12}C/^{13}C$ ratio larger than 500, and the other with $^{12}C/^{13}C$ ratio about 10. It was proposed by Vanture (1992a) that CH stars can also be divided into two classes with different $^{12}C/^{13}C$ ratios, one of which is characterized by $^{12}C/^{13}C \sim 3$ (near the equilibrium value of the CN cycle) and the other by $^{12}C/^{13}C \geq 25$. We didn't find such classes but rather a continuous distribution around $^{12}C/^{13}C \sim 10$ in most of CH stars, while another group has much larger $^{12}C/^{13}C$ ratio.

It is well known that the carbon stars of population I are also divided into two types, one with very low $^{12}C/^{13}C$ ratios (J-type) and the other with relatively high values (N-type). The $^{12}C/^{13}C$ ratios for these carbon stars have been by no means well established. A recent analysis of a large sample of N type stars, also based on the OAO data, revealed that the $^{12}C/^{13}C$ ratios are mostly between 20 and 30 with the mean value of 27±11 (std. dev.) for 62 N-type stars (Ohnaka & Tsuji 1996) while much higher values have been suggested before (e.g. $30 < {}^{12}C/^{13}C < 70$ derived by Lambert et al. 1986). Though the sample of CH stars is small yet, the distribution of $^{12}C/^{13}C$ of CH stars is obviously different from that of population I carbon stars. Two types can be found in the distribution of $^{12}C/^{13}C$ ratios for CH stars as well as for carbon stars of population I, but one of the types has much higher $^{12}C/^{13}C$ ratio ($\simeq$ 500) than N-type stars and the other has $^{12}C/^{13}C$ ratio of about 10, which is not found both in N-type and J-type stars. Furthermore, CH stars which

Table 7. Comparisons with other authors

Author	Star	result[a]		This work[a]
Kipper & Jørgensen (1994)	HD187216	7 (CN,SS)		10 (CN,COG)
Vanture (1992a)	HD198269	4 (C_2,SS)	6 (CN,SS)	7 (CN,COG)
	HD224959	3 (C_2,SS)	13 (CN,SS)	7 CN,COG)
	HD26	$>$25 (C_2,SS)	$\geq$25 (CN,SS)	10 (C_2,SS)
	HD201626	25 (C_2,SS)	$\geq$25 (CN,SS)	40 (C_2,SS)
Kipper (1992)	TT CVn	50$\sim$90 (C_2,SS)		$\geq$500 (C_2,SS)

[a] 'SS' and 'COG' means the spectral systhesis method and the curve-of-growth method, respectively.

show higher $^{12}C/^{13}C$ ratio are minor part of CH stars, while N-type stars which show relatively high $^{12}C/^{13}C$ ratio are the major part of population I carbon stars.

It may be useful to compare the $^{12}C/^{13}C$ ratios of CH stars with those of barium (Ba) stars, which are the red giants of population I whose atmospheres are enriched by carbon and s-process elements. These enhancements are considered to be the result of mass transfer from the AGB primary which was probably a cool carbon star and has already evolved to a white dwarf. The $^{12}C/^{13}C$ ratios in most of Ba stars are about 10 (Barbuy et al. 1992) which is much the same as that of the low $^{12}C/^{13}C$ group in CH stars. The relation between CH stars and Ba stars is discussed in the next section.

From the point of view of the binary mass transfer model (see Sect. 1) a comparison of CH stars with AGB stars is preferable as done above in this section. On the other hand, it will be also useful to compare the $^{12}C/^{13}C$ ratios of CH stars with those of population II RGB stars, because carbon stars are considered to have evolved through RGB phase. The distributions of $^{12}C/^{13}C$ in metal-poor RGB stars derived by many authors are summarized in Fig. 11, which includes both field giants (Sneden et al. 1986) and giants in globular clusters (Bell et al. 1990, Briley et al. 1994, Brown & Wallerstein 1989, Brown et al. 1991, Smith & Suntzeff 1989, Suntzeff & Smith 1991). Most of the effective temperatures of these stars are between 3800K and 5000K which are similar to those of the CH stars we have analysed. This distribution of metal-poor RGB stars shows a peak at $^{12}C/^{13}C = 3 \sim 4$ which is the equilibrium value of the CN cycle. We find that the distribution of $^{12}C/^{13}C$ ratio in low $^{12}C/^{13}C$ group of CH stars show a peak at $^{12}C/^{13}C \sim 10$, which is higher by about a factor of 3 than that of the metal-poor RGB stars.

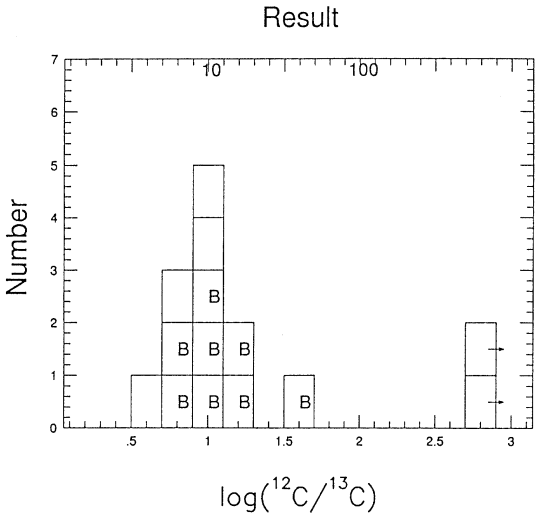

Fig. 10. The distribution of $^{12}C/^{13}C$ ratio for CH stars. The symbol 'B' implies that the star is binary, and two arrows of high $^{12}C/^{13}C$ group imply that the $^{12}C/^{13}C$ ratios are lower limit.

5.2. Evolution of carbon stars in the Galactic halo

5.2.1. Very high $^{12}C/^{13}C$ group

Simple estimations of carbon enhancement during the AGB evolution are tried for carbon stars of both populations I and II. We assume that the progenitor of a population I carbon star initially has carbon abundance of X ($\equiv$C/H), $^{12}C/^{13}C = 10$ and C/O = 0.5, while a population II star initially has carbon abundance X/10 or X/100, $^{12}C/^{13}C = 5$ and C/O = 0.25, where we adopt $^{12}C/^{13}C$ and C/O of normal giant stars and take into account that oxygen is relatively more abundant for a given metallicity and $^{12}C/^{13}C$ is lower (see Fig. 11) in metal-poor stars. Then we assume that ^{12}C increases by 2X in stars of both population by the 3rd dredge-up since ^{12}C production by 3α reaction is probably independent of metallicity. These assumptions and the results are summarized in Table 8. Notice that the predicted surface ratios of population II star show very high $^{12}C/^{13}C$ ratio and the $^{12}C/^{13}C$ ratio is higher for the stars with lower metallicity. The group of high $^{12}C/^{13}C$ ratio in CH stars can be accounted for by such a simple model of population II carbon star.

The formation of metal-poor carbon stars and their surface chemical compositions were calculated theoretically by Renzini & Voli (1981), where both convective dredge-up and nuclear burning in the deepest layers of the convective envelope (hot bottom burning) were considered. While the former dredges up fresh ^{12}C to the surface and $^{12}C/^{13}C$ ratio increases, the latter converts ^{12}C to ^{13}C and $^{12}C/^{13}C$ ratio decreases. They have shown that the very high $^{12}C/^{13}C$ ratio ($>$400) can be realized

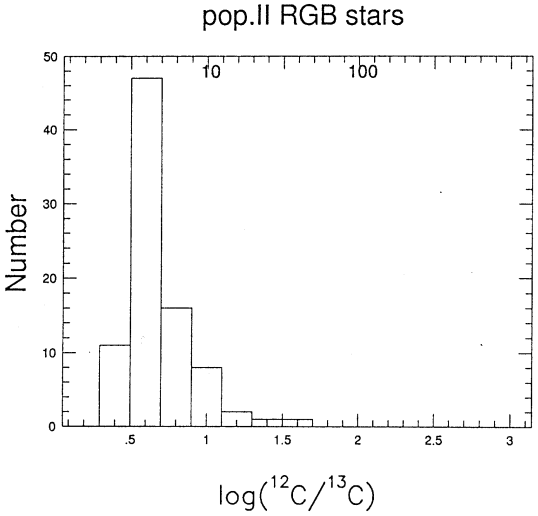

Fig. 11. The distribution of $^{12}C/^{13}C$ for metal-poor red giant branch stars. This is the simple sum of distributions of $^{12}C/^{13}C$ ratio derived by 7 works (see Sect. 5.1).

Table 8. Estimations of carbon enhancement during the AGB evolution

		RGB	3rd dredge-up	AGB	predicted
			^{12}C +2X		surface ratios
PopI	^{12}C:	X	→	3X	
	^{13}C:	X/10	→	X/10	$^{12}C/^{13}C$=30
	O:	2X	→	2X	C/O=1.5
PopII	^{12}C:	X/10	→	∼2X	
	^{13}C:	X/50	→	X/50	$^{12}C/^{13}C\simeq$100
	O:	4X/10	→	4X/10	C/O $\simeq$ 5
	^{12}C:	X/100	→	∼2X	
	^{13}C:	X/500	→	X/500	$^{12}C/^{13}C\simeq$1000
	O:	4X/100	→	4X/100	C/O $\simeq$ 50

in metal deficient stars (they calculated the case of Z=0.004) in the case that the hot bottom burning has not affected the surface chemical composition.

It is not clear whether V Ari and TT CVn are in AGB phase or not. The absolute magnitudes of V Ari and TT CVn are estimated about $M_{\rm bol} = -3.5$ by Eggen (1972b), but these are based on the assumption that these stars are on the giant branch of globular clusters. On the other hand, these stars are considered to be low-mass stars ($\leq 1M_{\odot}$) because they belong to the halo population. It is also not clear whether these low mass stars can become carbon stars by their own dredge-up of carbon or need the accretion of carbon-rich material from their companion. So far, there is no evidence that V Ari and TT CVn are binaries. Perhaps the fact that only two stars with very high $^{12}C/^{13}C$ ratio can be found may imply that most of these stars have already evolved to white dwarfs and V Ari and TT CVn are their rare remnants.

5.2.2. Low $^{12}C/^{13}C$ group

Explanation for the formation of the low $^{12}C/^{13}C$ group in CH stars cannot be so simple. It can be found that the peak of the distribution of $^{12}C/^{13}C$ ratio in the low $^{12}C/^{13}C$ group is higher than in oxygen-rich giants of population II (Figs. 10 and 11). This may reflect the supply of ^{12}C to the red giant by mass transfer from carbon rich companion. In this case, the ^{12}C supplied should be comparable with the initial ^{12}C abundance to transform $^{12}C/^{13}C$ ratio from ∼5 to ∼10. This is one possibility for formation of CH stars with low $^{12}C/^{13}C$ ratio. However this increase of ^{12}C will not be enough to change the oxygen-rich atmosphere to carbon-rich one because carbon abundance is smaller by factor 5 ∼ 10 than oxygen abundance in metal-poor RGB stars. Therefore this possibility seems to be small.

Another possibility for the formation of these CH stars is that the process of decreasing $^{12}C/^{13}C$ ratio, probably by the CN cycle, follows the large supply of ^{12}C. This is supported by the enhancement of nitrogen and the correlation between nitrogen abundance and $^{12}C/^{13}C$ ratio in CH stars shown by Vanture (1992b). Vanture (1992a,b) has proposed a model that ^{12}C rich material has been supplied by the accretion from the companion and mixed in the red giant branch by some mechanism which expose the accreted material to CN cycle and reduce the $^{12}C/^{13}C$ ratio. This model can be applied to our results for the low $^{12}C/^{13}C$ group, and is consistent with the fact that most of these stars are binaries as shown by McClure and Woodsworth (1990). This is nearly the same scenario as the formation of Ba stars (Barbuy et al. 1992). In Ba stars carbon enhancements are found even though most of Ba satrs show C/O<1. If the atmosphere of Ba star were metal-poor and then the oxygen abundance were small, carbon abundance would become larger than that of oxygen as in CH star. Hence the group of low $^{12}C/^{13}C$ ratio in CH stars may be the population II counterparts of Ba stars.

On the other hand, Renzini & Voli (1981) has shown that low $^{12}C/^{13}C$ carbon stars can be formed if the hot bottom burning affects the surface chemical composition. However, it seems necessary that the stellar initial mass is larger than $3M_{\odot}$ for the convective envelope burning, but it would not be possible for such massive stars to survive in the Galactic halo until the present. Therefore the mass transfer in the binary system should be considered again.

6. Concluding remarks

The carbon isotope ratios ($^{12}C/^{13}C$) of halo carbon stars (CH stars) are determined by observations of lines of CN red system and C_2 Swan band. Together with the previous results (Tsuji et al. 1991) and the present results, we obtain the distribution of $^{12}C/^{13}C$ ratio for 14 CH stars. Two groups regarding this ratio exist in CH stars. One of them is a group of very high $^{12}C/^{13}C$ ratio ($\geq$ 500) and the other is a group of rather low $^{12}C/^{13}C$ ratio (about 10), which includes most of stars. This distribution is different from that of population I carbon stars as well as from that of oxygen-rich RGB stars of population II. The stars with very high $^{12}C/^{13}C$ ratio can be explained by a simple model of

the increase of ^{12}C supplied by the 3α-process and third dredge-up, as in most of population I carbon stars (N-type). On the other hand the model of the formation of CH stars with low $^{12}C/^{13}C$ ratio may not be simple, as is the case of J stars which show low carbon isotopic ratios. Some ideas such as mass transfer in binary system or the hot bottom burning have been examined, but none is fully self-consistent.

So far, observational clues to the evolution of CH stars are rather meager because of the complexity of their spectra. Carbon isotopic ratio is one of the relatively well determined empirical constraints on the evolution of CH stars and their characteristic values, both high and low $^{12}C/^{13}C$ ratios found by us, should be explained by any theory of the evolution of CH stars. The situation is not much different for carbon stars of the disk population, but CH stars should have a unique importance to clarify the evolution of carbon stars, since it is known that the evolution of carbon stars depends on metallicity (Renzini and Voli 1981). It is also important to investigate the mass-loss of these stars as well as its dependence on metallicity. It is known that mass-loss plays an important role in the evolution of carbon stars in the Galactic disk. However there is little evidence for the existence of mass-loss in CH stars. Probably binary mass transfer may have played some role in mass-loss of CH stars and it is more difficult to investigate the mass-loss that took place long time ago. However, we expect that useful information about the circumstellar envelope will be brought by infrared spectra of CH stars which we hope to explore by the Infrared Space Observatory (ISO) for the first time.

On the other hand CH stars are important to clarify the chemical evolution of the early Galaxy as noted in the introduction (see Sect. 1). Generally speaking, to understand the contribution of intermediate and low mass stars to the Galactic chemical evolution is more difficult than that of high mass stars which explode as supernovae. For this purpose, understanding of the evolution of intermediate and low mass stars should be an important prerequisite. Unfortunately, however, evolution of CH stars, the major population (or its remnant) representing the intermediate mass stars in the Galactic halo, has not been established yet as we see above. Recently many ultra metal-poor stars with strong G-band have been found (Beers et al. 1992) and some of them may be CH stars or subgiant CH stars. This fact suggest that some of CH stars (or their progenitors) may be originating from the first generation of stars. The enhancement of s-process elements are known in CH stars as well as in carbon stars of the Galactic disk, while the heavy element abundances are found to be consistent with the r-process abundance pattern in most of very metal-poor stars (McWilliam et al. 1995). To clarify the origin of the s-process elements during the evolution of the Galaxy, it is certainly very useful to analyze the heavy element abundances, both r- and s- process elements, in CH stars and related objects in the sample of the ultra metal-poor stars, along with detailed chemical analyses of the classical CH stars.

Acknowledgements. We thank K. Ohnaka for sharing some experiences in observations and analyses during this work. We also thank R. L. Kurucz of Harvard-Smithsonian Center for Astrophysics for making available to us the latest CD-ROMs of his extensive line lists. Thanks are due to J. L. Greenstein for giving opportunities of observing at Mt. Wilson Observatory. Thanks are also due to G. Wallerstein for useful comments as a referee. We are grateful to T. Okada of OAO for his continuous support in observations. The OAO CCD system was developed by M. Iye in collaboration with E. Watanabe and other staffs of OAO. The data reductions and analyses were done by the use of the facilities of the Astronomical Data Analysis Center of NAOJ.

References

Amiot C., 1983, ApJS 52, 329
Barbuy B., Jorissen A., Rossi S.C.F., Arnould M., 1992, A&A 262, 216
Baushlicher C.W.Jr., Langhoff S.R., Taylor P.R., 1988, ApJ 332, 531
Beers T.C., Preston G.W., Shectman S.A., 1992, AJ 103, 1987
Bell R.A., Briley M.M. and Smith G.H., 1990, AJ 100, 187
Blackwell D.E., Petford A.D., Shallis M.J., 1980, A&A 82, 249
Blackwell D.E.,Leggett S.K., Petford A.D., Mountain C.M., Selby M.J., 1983, MNRAS 205, 897
Briley M.M., Smith V.V., Lambert D.L., 1994, ApJ 424, L119
Brown J.A., Wallerstein G., 1989, AJ 98, 1643
Brown J.A., Wallerstein G., Oke J.B., 1991, AJ 101, 1693
Cayrel R., Jugaku J., 1963, Ann. d'Astrophys. 26, 495
Davis S.P., Phillips J.G.,1963, 'The Red System of the CN Molecule', Univ. of California Press, Berkeley
Danylewych L.L., Nicholls R.W., 1974, Proc.R.Soc.Lond.A. 339, 197
Dominy J.F., 1984, ApJS 55, 27
Dominy J.F., Lambert D.L., Gehrz R.D.,, Mozurkewich D., 1986, AJ 91, 951
Earls L.T., 1935, Phys.Rev. 48, 423
Eggen O.J., 1972a, MNRAS 159, 403
Eggen O.J., 1972b, ApJ 174, 45
Feast M.W.,, Whitelock P.A, 1992, MNRAS 259, 6
Fuhr J.R., Martin G.A., Wiese W.L., 1988, J. Phys. Chem. Ref. Data 17, Suppl. No.4
Gezari D.Y., Schmitz M., Pitts P.S. Mead J.M., 1993, 'Catalog of Infrared Observations', 3rd ed., NASA Ref. Publ. 1294
Hartwick F.D.A., Cowley A.P., 1985, AJ 90, 2244
Huber K.P., Herzberg G., 1979, 'Constants of diatomic molecules', Van Nostrand Reinhold Company
Keenan P.C., 1942, ApJ 96, 101
Keenan P.C., 1993, PASP 105, 905
Kipper T., Jørgensen U.G., 1994, A&A 290, 148
Kipper T., 1992, Baltic Astronomy 1, 181
Kurucz R.L., Bell B., 1995, 'Kurucz CD-ROM No. 23' Smithsonian Astrophysical Observatory
Lambert D.L., Gustafsson B., Eriksson K. and Hinkle K.H., 1986, ApJS 62, 373
McClure R.D., Woodsworth A.W., 1990, ApJ 352, 709
McWillam A., Preston G.W., Sneden C., Searle L., 1995, AJ 109, 2757
Meggers W.F., Corliss C.H., Scribner B.F., 1975, NBS Monograph 145
Naulin C., Costes M., Dorthe G., 1988, Chemical Physics Letters 143, 496
Ohnaka K., Tsuji T., 1996 A&A 310, 933
Pesic D.S., Vujisic B.R., Rakotoarijimy D., Weniger S., 1983, Jounal of Molecular Spectroscopy 100, 245
Phillips J.G., Davis S.P., 1968, 'The Swan System of the C_2 Molecule', Univ. of California Press, Berkeley

Renzini A., Voli M., 1981, A&A 94, 175
Schadee A., 1967, J. Quantit. Spectrosc. Radiat. Transfer 7, 169
Smith V.V., Suntzeff N.B. 1989, AJ 97, 1699
Sneden C., Pilachowski C.A., Vandenberg D.A., 1986, ApJ 311, 826
Suntzeff N.B., Smith V.V. 1991, ApJ 381, 160
Tsuji T., Iye M., Tomioka K., Okada T., Sato H., 1991, A&A 252, L1
Vanture A.D., 1992a, AJ 103, 2035
Vanture A.D., 1992b, AJ 104, 1986
Vanture A.D., 1992c, AJ 104, 1997
Wallerstein G., Greenstein J.L., 1964, ApJ 139, 1163
Wyller A.A., 1966, ApJ 143, 828

Note added in proof: After the manuscript was completed we learned during the IAU symposium 177 'The carbon star phenomenon' (May 1996, Antalya) that HD85066 was confirmed to be binary by R. D. McClure. This information is included in Fig. 10.

This article was processed by the author using Springer-Verlag LaTeX A&A style file *L-AA* version 3.